

# A SLOPE-BASED TECHNIQUE FOR MOTION ESTIMATION AND OPTIMUM TIME SELECTION FOR ISAR IMAGING OF SHIP TARGETS

Debora Pastina<sup>(1)</sup>, Chiara Spina<sup>(2)</sup>, and Angelo Aprile<sup>(3)</sup>

<sup>(1)</sup> INFOCOM Dpt., University of Rome "La Sapienza", Via Eudossiana 18, 00184 Rome, Italy  
phone: + 39-0644585860, fax: +39-064873300, email: [debora@infocom.uniroma1.it](mailto:debora@infocom.uniroma1.it)

<sup>(2)</sup> Selex Airborne and Sensor Systems - Galileo Avionica Spa, Via dei Castelli Romani 2, 00040 Pomezia (Rome) – Italy,  
email: [chiara.spina@galileoavionica.it](mailto:chiara.spina@galileoavionica.it)

<sup>(3)</sup> Selex Airborne and Sensor Systems - Galileo Avionica Spa, Via G.B. Grassi 93, 20157 Milan – Italy,  
email: [angelo.aprile@galileoavionica.it](mailto:angelo.aprile@galileoavionica.it)

## ABSTRACT

*The focus of this paper is on optimum time selection and angular motion estimation for ship ISAR imaging. The aim is to select proper imaging intervals and to estimate ship angular motion in order to obtain high quality top-view or side-view ship images suitable for processing by classification/identification procedures. To this purpose a slope-based ISAR algorithm is proposed, able to estimate the time instants better suited for top or side-view image formation and the rotation motion vertical/horizontal components for image scaling. The performance of the proposed ISAR technique is investigated against simulated data under different ship model, ship motion, acquisition geometry and background conditions. Results obtained by applying the proposed technique to live ISAR data proves the effectiveness of the proposed approach.*

## 1. INTRODUCTION

This paper deals with the problem of Inverse Synthetic Aperture Radar (ISAR) imaging of multi-scatterer ship targets. Medium/high resolution (about 1 meter or less) target images can be obtained by using the ISAR technique [1]: a wide bandwidth waveform is transmitted to achieve fine range resolution; coherently processing the echoes returned from the target at different aspect angles gives fine cross-range resolution. In ISAR the angular aperture under which the target is viewed by the radar is due to the motion of the target itself.

Particularly, for ship targets, the ship angular motion around its centre of gravity is dominant with respect to translation motion and usually larger than needed to achieve the desired cross-range resolution. Thus ship images are obtained by properly using this ship angular motion. In order to get well-focused images the instantaneous radar-target distance, and therefore the target motion, must be exactly known. Moreover, the orientation of the Image Projection Plane (IPP) depends itself on the target motion, [2], being the IPP normal to the effective rotation rate vector (the rotation rate component normal to the Line Of Sight, LOS). High quality images can be obtained when the rotation axis is almost fixed during time aperture. In particular, top-view images arise from ship targets rotating around a vertical axis (the effective rotation vector has

only a vertical component), while side-views from ship targets rotating around an horizontal axis (the effective rotation vector has only an horizontal component). Therefore the knowledge of the ship rotation motion, decoupled in horizontal and vertical components, allows us to know the orientation of the IPP and, more specifically, to select proper imaging intervals in order to achieve high quality scaled images on a proper IPP as top-view or side-view images (the most useful for classification/ identification, [3]). Since the ship navigation data are usually unknown, the information relevant to time selection and image focus/scale must be estimated directly from the received radar signal. The estimation of ship angular motion directly from radar data is therefore of great importance for both non-cooperative targets classification/ identification and vessel traffic management, allowing a complete real-time control, surveillance and traffic management in wide sea areas.

In the present paper we focus on the problem of selecting proper imaging intervals and estimating the ship rotation motion and we propose a new technique in order to select the suitable imaging times and to estimate both the vertical and horizontal rotation motion components.

## 2. TARGET MODEL

The ship target model used in this paper is the one proposed in [5]: the main concepts are here briefly summarized.

The operative condition is given by a radar system transmitting a wide bandwidth pulsed waveform and by a ship target undergoing a rotation about its centre of mass (target fulcrum). We assume already compensated any translation motion between the radar antenna and the ship reference point. Usually the rotation motion is taken into account by introducing the yaw, pitch and roll rotation motions defined as the rotation around respectively the ship vertical axis, the ship width and the ship length.

In our target model different reference systems are considered. The body reference system ( $O', X_b, Y_b, Z_b$ ) has origin on the ship reference point and is assumed integral with the target: in particular the  $X_b$ ,  $Y_b$  and  $Z_b$  axes represent respectively the ship length, width and height. The ( $O', R, H, V$ ) reference system is centred on the ship fulcrum, with  $R$  axis ( $\hat{r}$  unitary vector) representing the LOS direction,  $H$  axis given by the unitary vector  $\hat{h}$  normal to  $\hat{r}$  and belonging to

the ( $X_b$ - $Y_b$ ) plane and finally the V axis given by the unitary vector  $\hat{v}$  normal to the (R,H) plane.

We assume the ship characterized by N dominant scatterers, each with complex reflectivity constant during the time aperture and fixed coordinates,  $[x_b^n, y_b^n, z_b^n]$  for n-th scatterer, in the ( $O', X_b, Y_b, Z_b$ ) reference system. As shown in [5], around a generic time  $t_0$  we can assume the scatterer with coordinates  $[r_0^n, h_0^n, v_0^n]$  rotating around H and V axes (rotation around R axis is not considered since the radar is not sensitive to rotations around its LOS, [2]). If  $\varrho_v(t)$  is the angle, changing with time, swept around V axis and  $\varrho_h(t)$  is the angle, changing with time, swept around H axis, around  $t_0$  we have at first order for the Doppler frequency of the n-th scatterer:

$$f_d^n(t) \cong -\frac{2}{\lambda} \left[ (v_0^n \dot{\omega}_{h_0} - h_0^n \dot{\omega}_{v_0}) + (v_0^n \dot{\omega}_{h_0} - h_0^n \dot{\omega}_{v_0}) \cdot (t - t_0) \right] \quad (1)$$

with  $\omega_{v_0} = \dot{\varrho}_{v_0} = \dot{\varrho}_{v_0}(t_0)$ ,  $\dot{\omega}_{h_0} = \dot{\varrho}_{h_0} = \dot{\varrho}_{h_0}(t_0)$  and  $\omega_{h_0} = \dot{\varrho}_{h_0} = \dot{\varrho}_{h_0}(t_0)$ ,  $\dot{\omega}_{v_0} = \ddot{\varrho}_{v_0} = \ddot{\varrho}_{v_0}(t_0)$ .

The coordinates  $[r_0^n, h_0^n, v_0^n]$ , are written as, [5]:

$$\begin{aligned} r_0 &= \cos(\psi) \cos(\xi_0) x_b - \cos(\psi) \sin(\xi_0) y_b + \sin(\psi) z_b \\ h_0 &= -\sin(\xi_0) x_b - \cos(\xi_0) y_b \\ v_0 &= \sin(\psi) \cos(\xi_0) x_b - \sin(\psi) \sin(\xi_0) y_b - \cos(\psi) z_b \end{aligned} \quad (2)$$

where  $\psi$  is the grazing angle and  $\xi$  is the target aspect angle, i.e. the angle between LOS and  $X_b$  axis. Eqs. (1-2) show that, in general, both  $\omega_{v_0}$  and  $\omega_{h_0}$  contribute to the scatterer phase/frequency. Nevertheless it is apparent that scatterers belonging to the deck will be more affected by  $\omega_{v_0}$  ( $v_0^n \ll h_0^n$ ) while scatterers from superstructures will be more affected by  $\omega_{h_0}$  ( $v_0^n \gg h_0^n$ ), [3].

### 3. SLOPE-BASED TECHNIQUE

We assume the radar echoes backscattered by the ship acquired from time  $t=0$  to a generic time  $t=T_{\max}$  and refer to radar signal after range compression. The acquired radar signal is processed by successive time batches, separated or partially overlapped ( $T_b$  batch length).

In order to select proper imaging intervals the technique proposed in this paper works as follows: on a batch by batch basis 1) the acquired radar signal is pre-processed to obtain a pseudo-segmented image of the ship with the ship segment defined as the polygon containing all the detected ship scatterers; 2) several linear features (including ship centerline, deck line and mainmast axis) of the ship image are estimated to evaluate the portion of the ship segment due to the side-view projection and the portion due to the top projection; 3) the estimated slope (Hz/m) of the ship centreline and of the mainmast axis in the slant-range/Doppler-frequency plane are then used to estimate the vertical and horizontal motion components. It is apparent that results of step 2 are used to select the optimum imaging time while results of step 3 are used to correctly scale the ship image.

Details of the above processing steps are given below.

#### 1) Pre-processing

In order to obtain the pseudo-segmented image the pre-processing consists of the following steps: (a) obtain the weighted and oversampled ship image in the slant-range/Doppler-frequency domain via FFT (Fast Fourier Transform); (b) clear the image from disturbance spikes in order to localize the ship scatterers; (c) select the polygon which includes all the ship scatterers; (d) detect the ship segment edges. Obviously the ISAR technique proposed in this paper can also be applied to the segmented image obtained by using more complex and accurate segmentation procedures as in [4].

#### 2) Top and side-view components estimation

The estimate of the top and side-view components of the segmented image is obtained by means of the following steps: (a) estimate the ship centreline axis, [4], defined as the line through bow and stern; (b) as the centreline divides the ship segment into two parts, distinguish the superstructure portion containing the side-view projection (i.e. the projection of the superstructure) from the body portion containing the deck; (c) find the first deck-line defined as the line parallel to the ship centreline and tangent to the body portion and take as the second deck-line that line belonging to the superstructure portion and specular to the first deck-line w.r.t. the ship centreline; (d) evaluate the top component as the portion of the ship segment between the two deck-lines; (e) evaluate the side view component as the portion complementary to the top component.

#### 3) Vertical/horizontal rotation components estimation

The estimation of the slopes (Hz/m) of the ship centreline and of the mainmast axis (both estimates in the range-Doppler plane based on the Radon transform) can be used to estimate the vertical and horizontal components of the rotation motion. Based on the target model in Section 2 it could be shown that the ship centreline slope (Hz/m) in the slant-range/Doppler frequency plane at any  $t_0$  is given approximately by

$$m_{//}(t_0) = -\frac{2}{\lambda} \left[ \tan(\psi) \omega_{h_0} + \frac{1}{\cos(\psi)} \tan(\xi_0) \omega_{v_0} \right] \quad (3)$$

while for the mainmast axis slope we have

$$m_{\perp}(t_0) = \frac{2}{\lambda} \frac{\omega_{h_0}}{\tan(\psi)} \quad (4)$$

The following observations apply: (i) when  $\psi \approx 0$   $m_{//}$  depends only on  $\omega_{v_0}$  and  $m_{\perp} \rightarrow \infty$  therefore it is possible to estimate  $\omega_{v_0}$  but not  $\omega_{h_0}$ : in this case we achieve scaled top-views and unscaled side-views; (ii) when  $\psi$  is not negligible (for example at short range) both  $\omega_{v_0}$  and  $\omega_{h_0}$  can be evaluated from the estimated slopes by using eqs. (3-4): in this case it is possible to scale both top and side-views.

### 4. PERFORMANCE ANALYSIS

The performance of the slope-based ISAR technique is tested first against simulated radar data. In particular a multi-scatterer ship model is considered with length of about 120 m,

width of about 16 m, mainmast height 35 m above the deck level and with more than 200 interfering scatterers. The assumed ship model could be representative of a large and complicated ship such for example a frigate.

The transmitted bandwidth is set to 100-300 MHz (in order to achieve 1.5-0.5 m slant-range resolution),  $\lambda=0.03$  m and the PRF is set to 1 KHz. Concerning the acquisition geometry we consider both cases of negligible grazing ( $\psi=0^\circ$ ) and not negligible grazing ( $\psi=10^\circ$ ) while the aspect angle  $\xi_0$  is set to  $45^\circ$ . Different motion conditions have been considered: sinusoidal yaw (yaw: with amplitude  $A_y=1^\circ$  and frequency  $f_y=0.21$  Hz), sinusoidal pitch&roll (pitch with  $A_p=1^\circ$  and  $f_p=0.178$  Hz and roll with  $A_r=5^\circ$  and  $f_r=0.091$  Hz) and finally yaw&pitch&roll. The proposed algorithm has been applied on a batch-by-batch basis with  $T_b=0.256$  sec and 50% overlap between consecutive batches. Both noise-free ( $\text{SNR}=\infty$ ) and noisy ( $\text{SNR}=25$  dB in the image domain, for white Gaussian background) conditions have been considered. It is to be noticed that disturbance-free conditions are of interest because, even in absence of a background contribution, the performance can be highly degraded by the interference among the different ship scatterers.

As an example Fig.1 shows the original ISAR image of the ship under consideration, the detected scatterers, the peaks of the detected scatterers and the pseudo-segmented image at a given batch.

Fig. 2 shows the results of the top and side projection components estimation for the case of sinusoidal yaw, pitch and roll, resolution 1.5 m and  $\psi=0^\circ$ : as apparent from the figure optimum imaging times providing top or side views are clearly localized. Similar results could be shown for the cases of sinusoidal yaw motion only and sinusoidal pitch and roll as well as for the case  $\psi=10^\circ$ . Fig. 3 shows the results of the estimate of the vertical component of the motion for the case resolution 1.5 m,  $\psi=10^\circ$  and yaw only (top) and yaw&pitch&roll (bottom). In all the considered cases the proposed centreline slope based technique is able to estimate  $\omega_v$  with a mean normalized error (averaged over all the batches) less than about 13%: obviously in the yaw&pitch&roll the performance is worst if compared with the yaw case due to the influence of horizontal component. In particular in the yaw&pitch&roll case we have for  $\psi=10^\circ$  a normalised mean error of about 13% whereas for  $\psi=0^\circ$  we have about 6%; in the yaw only case, regardless the grazing value, the mean error is less than 5%.

Figs. 4-5 show the results of the estimate of the horizontal component of the motion for both resolutions 0.5 m and 1.5 m,  $\psi=10^\circ$  and pitch only (Fig.4) and yaw&pitch&roll (Fig.5). As stated in the previous section the estimate of  $\omega_h$  can be obtained only in presence of a not negligible grazing angle (short range): in this case obviously the best performance is obtained in the pitch&roll case and by using high range resolution which allows to better resolve in the range direction the mainmast and the different element of the superstructure. In particular the mean normalized error is about 20% in the yaw&pitch&roll case while it decreases to about 10% in presence of pitch&roll only.

The above results show that the proposed technique allows to select the proper imaging times and to scale the selected images with a small percentage error thanks to the good per-

formance of the motion estimation techniques. As an example by selecting the batches at about 2.2 and 3.5 seconds the ship images in Fig. 6a-b are obtained which are also scaled accordingly to the estimated values of the rotation rate components.

| <b><math>\omega_v</math> &amp; <math>\omega_h</math> estimation performances<br/>(SNR = 25 dB, aspect <math>45^\circ</math>, 10 seconds, smoothed data)</b> |  |  |
|---|--|--|
| <b>Motion - Geometry -<br/>Bandwidth</b>  | $\left\langle \left  \frac{\hat{\omega}_v - \omega_v}{\omega_v} \right  \right\rangle$ | $\left\langle \left  \frac{\hat{\omega}_h - \omega_h}{\omega_h} \right  \right\rangle$ |
| <b>Yaw&amp;Pitch&amp;Roll</b><br>$\Psi=0^\circ, B=100$ MHz  | 0.05   | -----  |
| <b>Yaw&amp;Pitch&amp;Roll</b><br>$\Psi=10^\circ, B=100/300$ MHz   | 0.12 / 0.09  | 0.23 / 0.15  |

Table 1: Normalized estimation errors analysis for SNR = 25 dB.

The proposed estimation technique is also very robust to the presence of a background provided that the ship segment is acceptably recognized since the technique works in the image domain (after azimuth integration) without requesting Doppler tracking or phase estimation of ship scatterers. Fig. 7 shows the mean top and side projection components estimated for the case of sinusoidal yaw, pitch and roll, resolution 1.5 m and  $\psi=0^\circ$  with a SNR=25 dB: the results are obtained by averaging over 100 different background realizations. As apparent the results obtained in the noisy conditions closely follows the behaviour in noise free conditions. The normalized mean errors obtained in the same conditions are shown in Table 1. These results are obtained by averaging over all the batches and over 100 different realizations of the background noise. As evident the performance obtained in the noisy case are of the same order of the values obtained in noise free conditions thus showing the effectiveness of the proposed approach.

## 5. APPLICATION TO LIVE ISAR DATA

The above-described technique has been applied to an extensive amount of live data acquired by more than 10 flights from February to December 2002 against co-operative and non-cooperative ship targets. Fig. 8 depicts the system employed for the flight trials (Aircraft: Sabreliner T39-A and Radar: X-Band Coherent Pulse Doppler Radar). Validation of presented ISAR algorithm through live data, demonstrates that estimation of ship centreline slope and Doppler spread represent the keys for target motion estimation and best imaging time selection.

Fig. 9 reports the top and side projection components, the centreline slope, the Doppler spread as estimated by applying the proposed technique to radar data of a non co-operative commercial ship acquired by the above radar system over a time interval of about 18 seconds. For the considered radar data set the transmitted bandwidth is 200 MHz (0.75 m slant-range resolution). The ship was located at about 30 Km from the radar and observed with grazing angle 3.30 degrees and initial aspect angle 15.5 degrees. Note that the small centreline slope values are basically due to the low aspect angle while the low Doppler spread values indicates a relatively calm sea state. The behaviour of the estimated centreline slope in Fig. 9 indicates the presence of a small vertical component. Best time instants for side-view imaging are selected by choosing time instants

with a high Doppler spread and a close to zero vertical component: Fig. 10 shows the ship side-view image, not scaled, obtained at time  $\approx 15.8$  sec with synthetic aperture 2 sec. The agreement of the results obtained for real and simulated data indicates that the performance prediction shown in the previous Section is representative of the performance achievable in a practical application of the new proposed ISAR algorithm.

**ACKNOWLEDGEMENT**

This work has been supported by Galileo Avionica Spa, Radar Systems Business Unit, Milan (Italy).

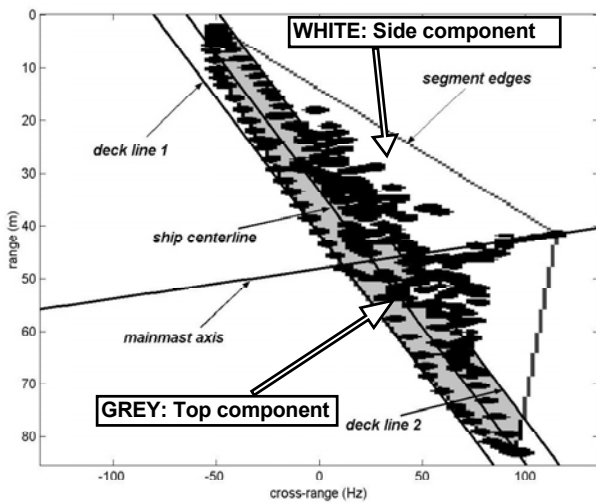


Figure 1 - Example of batch processing results.

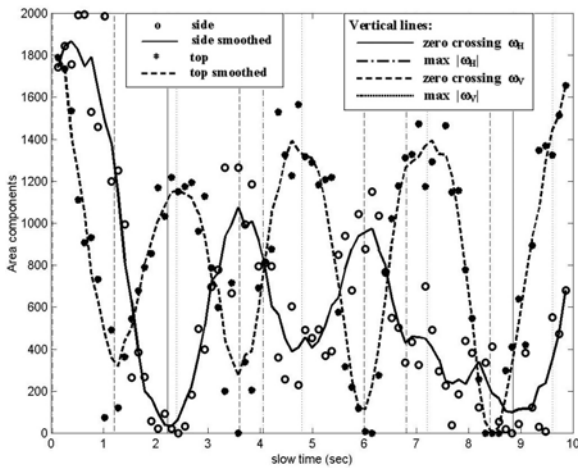


Figure 2 - Top and side projection vs. slow time for the case yaw&pitch&roll,  $\psi=0^\circ$ ,  $\xi_0=45^\circ$ .

**REFERENCES**

[1] J.L. Walker, "Range-Doppler imaging of rotating objects", *IEEE Trans. on AES*, Vol. 16, No.1, 1980, pp.23-52.  
 [2] D.R. Wehner, "*High-Resolution Radar*", Artech House, Boston, 1995.  
 [3] A.W. Rihaczek, S.J. Hershkowitz, "*Theory and practice of radar target identification*", Artech House, Boston, 2000, Chapter 5.  
 [4] S. Musman, D. Kerr, C. Bachmann, "Automatic recognition of ISAR ship images", *IEEE Trans. On AES*, Vol. 32, No. 4, 1996, pp. 1392-1404.  
 [5] D. Pastina, A. Montanari, A. Aprile: "Motion estimation and optimum time selection for ship ISAR imaging", *Proc. Of RADAR 2003*, Huntsville, Alabama, USA, May 2003, pp.7-14.

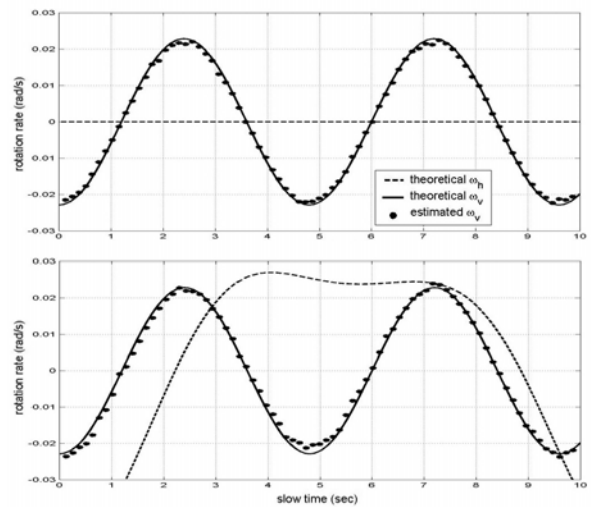


Figure 3 - True and estimated  $\omega_v$  component vs. slow time for the case  $\xi_0=45^\circ$  and  $\psi=10^\circ$ , yaw (top) and yaw&pitch&roll (bottom).

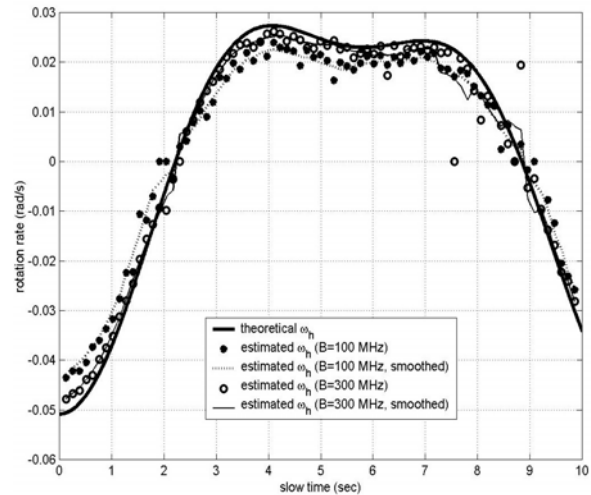


Figure 4 - True and estimated  $\omega_h$  component vs. slow time for the case pitch&roll, case  $\xi_0=45^\circ$  and  $\psi=10^\circ$ .

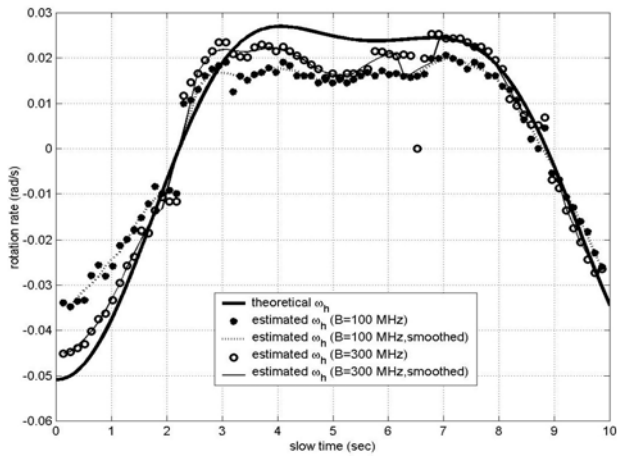


Figure 5 - True and estimated  $\omega_h$  component vs. slow time for the case yaw&pitch&roll,  $\xi_0 = 45^\circ$  and  $\psi = 10^\circ$ .

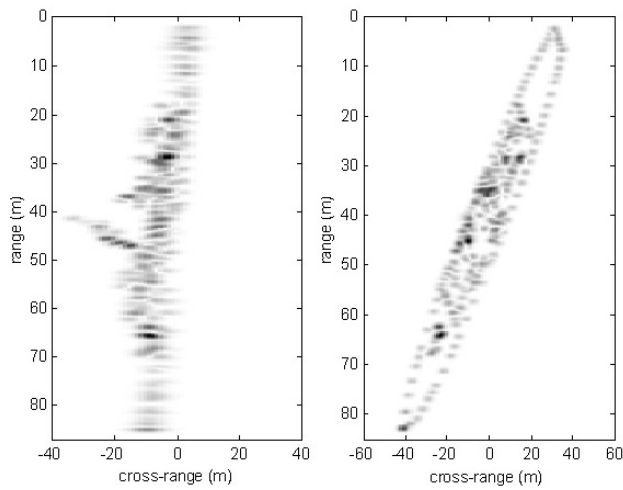


Figure 6 - Ship ISAR images at the selected time instants.

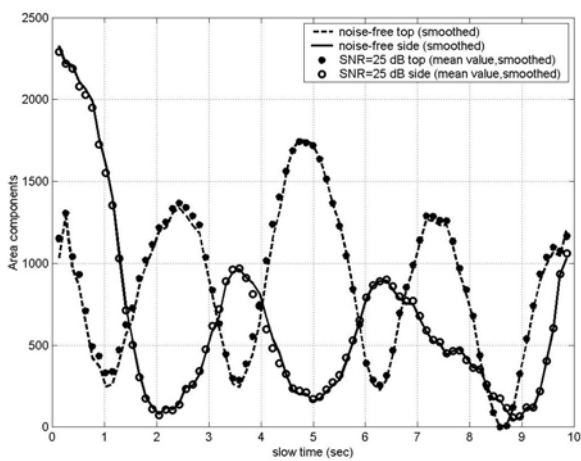


Figure 7 - Top and side projection vs. slow time for the case yaw&pitch&roll,  $\psi = 0^\circ$ ,  $\xi_0 = 45^\circ$ , SNR = 25 dB.



Figure 8 - System employed for live data acquisition

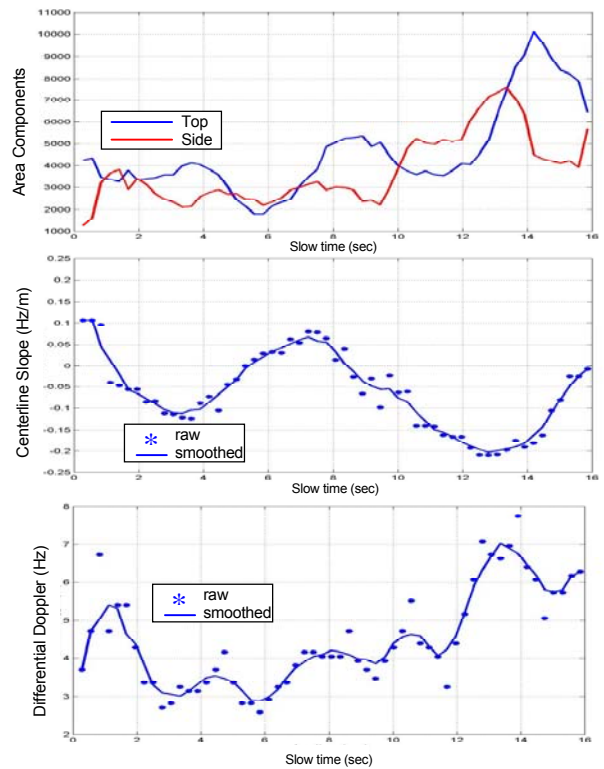


Figure 9 - Estimated top and side projections, centreline slope and Doppler spread versus slow-time for ship live ISAR data.

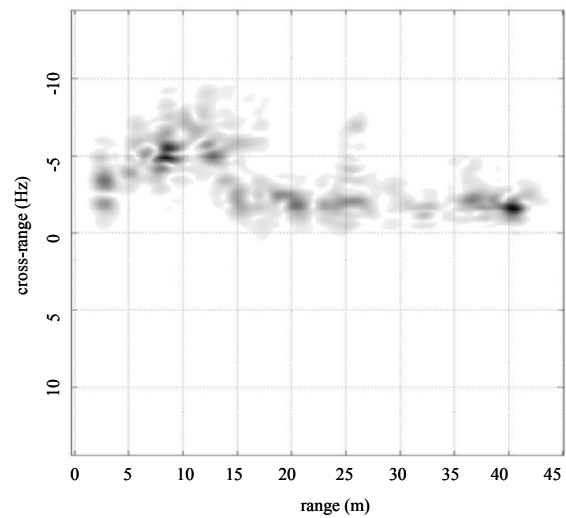


Figure 10 - Ship side-view image.